Physical principles of IR and Raman

- IR results from the absorption of energy by vibrating chemical bonds. Raman scattering results from the same types of transitions, but the selection rules are different so that weak bands in the IR may be strong in the Raman and vice versa.
- The precise wave numbers of bands depend on inter and intra molecular effects, including peptide-bond angles and hydrogen-bonding patterns.
- Nine normal modes are allowed for the amide band of proteins. These are called A, B, and I-VII in order of decreasing frequency.
- The amide bands I (80% C=O stretch, near 1650cm^{-1}), II (60% N–H bend and 40% C–N stretch, near 1550cm^{-1}), and III (40% C–N stretch, 30% N–H bend, near 1300 cm^{-1}) are generally employed to study protein structure.

Infrared Spectroscopy

The energies of photons in the far IR region of spectrum correspond to transitions between vibrational energy levels

In biology, IR spectroscopy is most commonly employed to quantitate secondary structure or to determine changes in these structures.

Number of vibrational transition.

A molecule with *N* atoms has 3*N* "*degrees of freedom*."

3 are translational
and 2 (if linear) or 3 (if nonlinear) are rotational
The remainder
3N-5, if linear;
3N-6, if non-linear are vibrational degrees of freedom.

IR spectroscopy

Transitions between a vibrational level and the next higher vibrational level (v ⇒ v+1) are strong

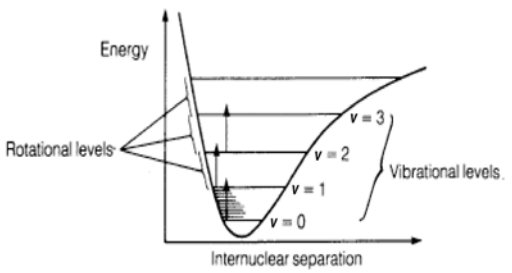

Based on the solution to the Schrödinger equation of the Harmonic Oscillator,

$$E_v = (v + \tfrac{1}{2})h\nu_0, \qquad where\ 2\pi\nu_0 = \left(\frac{k}{\mu}\right)^{1/2}$$

one would then predict that for each vibration one should observed one major absorption peak, and perhaps minor overtones of this corresponding to v ⇒ v+2

The actual picture is slightly more complicated than this.

IR spectrum of *trans*-retinal

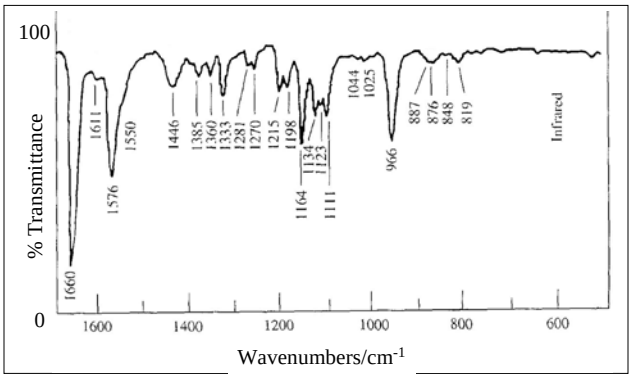

The % transmittance is the percent of incident light (I_0) that passes through the sample.

$$\% \text{ transmittance} = 100 \times (I / I_0)$$

Unlike absorbance, % transmittance is not additive, and thus the contributions due to impurities or solvent cannot be subtracted out. Thus these spectra cannot be used to determine concentrations, etc.

IR spectroscopy

The frequency is given in wavenumbers.

$$\bar{\nu} = \frac{\nu}{c}$$

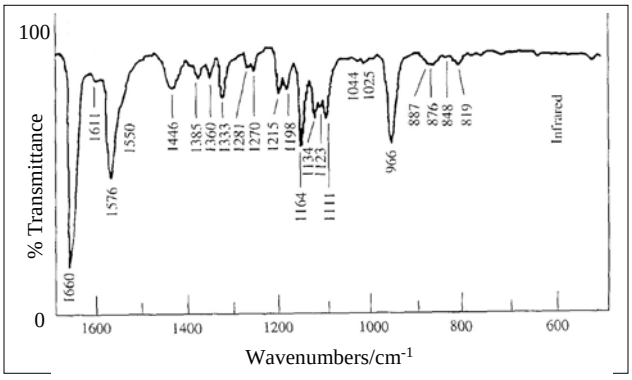

Each peak in the spectrum corresponds to a given vibration of the retinal molecule.

The number of expected peaks or modes of vibration for a given molecule can be calculated based on the number of atoms.

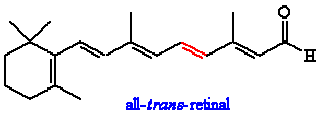

IR spectrum of N-methylacetamide.

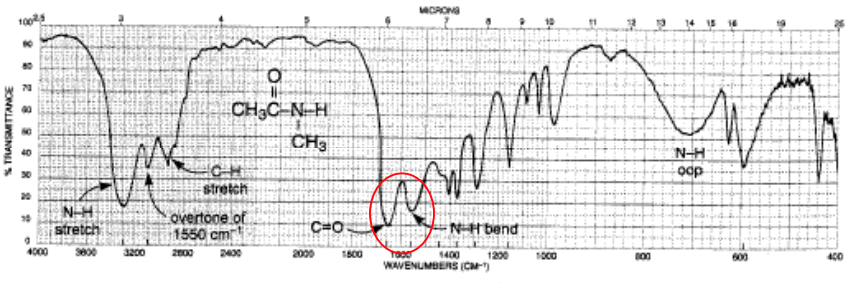

Note the strong band at ~1650.

The peaks stems from the amide carbonyl group.

Absorptions in this region are a general indication of either carbonyl, vinyl, or aromatic groups.

Not surprisingly, similar bands are found in peptides and proteins.

The model compound N-methylacetamide (NMA)

NMA is the smallest molecule that contains a trans-peptide group. It has therefore become the starting point for a normal mode analysis of polypeptide backbone vibrations.

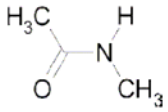

If the CH_3 groups are regarded as point masses, the number of atoms of NMA is 6 and thus there are 12 normal modes.

Only two side-chain moieties absorb in spectral regions that are free from overlapping absorption by other groups

These are the SH group of Cys (2550–2600 cm^{-1})
and the carbonyl group of protonated carboxyl groups (1710–1790 cm^{-1})

Useful when protonation and deprotonation of carboxyl groups is of interest, for example when proton pathways in proteins are explored

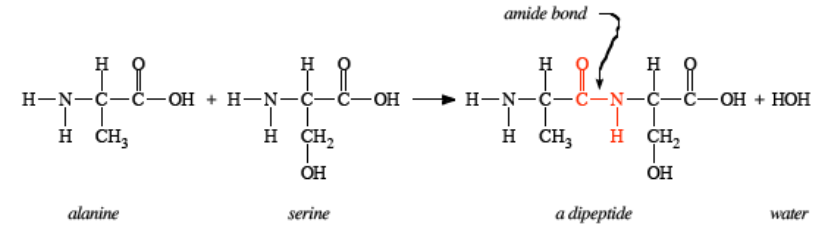

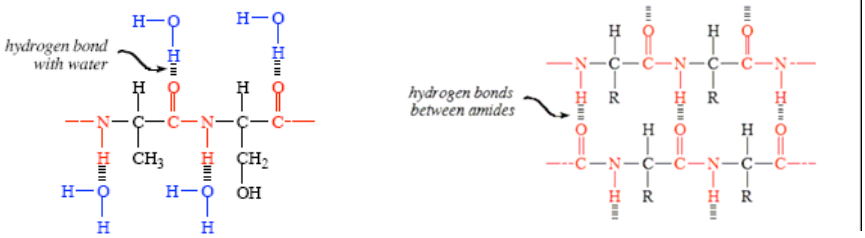

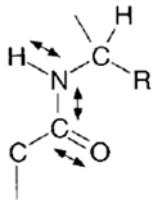

Normal modes

(selection)

SPECTRAL ANALYSIS BOX

AMIDES

C=O	Stretch occurs at approximately 1680–1630 cm^{-1}.
N—H	Stretch in primary amides (—NH_2) gives two bands near 3350 and 3180 cm^{-1}. Secondary amides have one band (—NH) at about 3300 cm^{-1}.
N—H	Bending occurs around 1640–1550 cm^{-1} for primary and secondary amides.

Major Group Vibrations: Protein Backbone

Amide bands reflect global conformational changes
Amides A and B (N-H stretch), 3100 and 3300 cm-1
Amide I (mostly C=O stretch), 1600-1700 cm-1

Often used to determine protein secondary structure, even though the correlation is **not absolute**:
α-helix is at 1648-1660 cm^{-1}
β-sheet is at 1625-1640 cm^{-1}
turns are at 1660-1685 cm^{-1}
Unordered peptides are at 1652-1660 cm^{-1}

Amide II (mostly N-H bend and C-N stretch), 1510-1580 cm^{-1}
very sensitive to H/D exchange, so it is often used (along with Amide I) to check solvent accessibility of the protein core and to distinguish between unordered and helical conformations

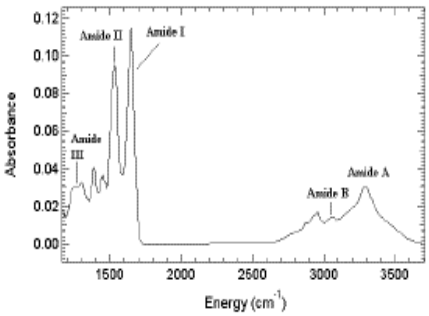

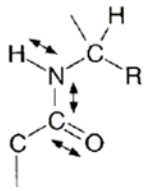

Normal modes

(selection)

Table 5.4 *Characteristic Infrared Bands of the Peptide Linkage*

Designation	Approximate frequency (cm^{-1})	Description
A	~3300	NH stretching in resonance with (2 × amide II) overtone
B	~3100	
I	1600–1690	C═O stretching
II	1480–1575	CN stretching, NH bending
III	1229–1301	CN stretching, NH bending
IV	625–767	OCN bending, mixed with other modes
V	640–800	Out-of-plane NH bending
VI	537–606	Out-of-plane C═O bending
VII	~200	Skeletal torsion

From H. Susi, *Methods Enzymol.* 26:455–472 (1972).

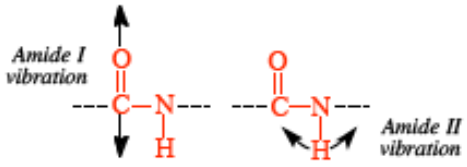

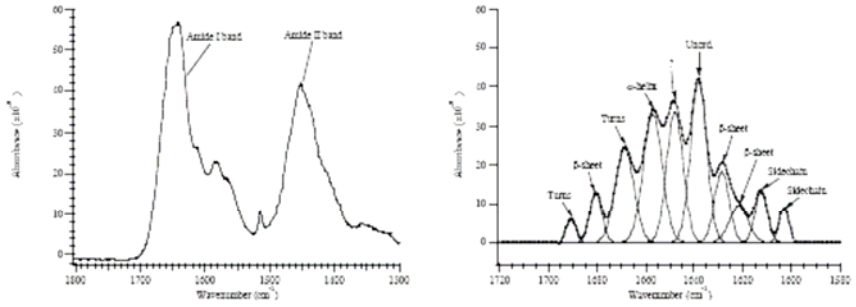

a. b.

The amide I band of polypeptides has long been known to be sensitive to secondary structure and this has caused considerable interest in the understanding of the structure–spectrum relationship.

Transition dipole coupling (TDC): fundamental mechanism that renders the amide I vibration sensitive to secondary structure is TDC.
A resonance interaction between the oscillating dipoles of neighbouring amide groups and the coupling depends upon the relative orientations of, and the distance between, the dipoles. Coupling is strongest when the coupled oscillators vibrate with the same frequency.

A fundamental problem is that the assignment of a given component band to a secondary structure type is not unique or straightforward.

Possible problems:
•overlap of α-helix and random structures in ^1H_2O,
•side bands of α-helices below 1650 cm^{-1} which are commonly assigned to β-sheets and give rise to errors for proteins with a large α-helical content,
•the absorption of bent helices below 1650 cm^{-1}
•the assignment of bands in only the 1660–1690 cm^{-1} region to turn structures although they are predicted to absorb in the entire amide I region (see previous section).

Hydrogen/deuterium exchange partly resolves this problem: for example the overlap of α-helix and random structure bands in ^1H_2O is greatly reduced in ^2H_2O.

Hydrogen/deuterium exchange leads to small band shifts of the amide I components. This is caused by the small contribution of the N—H bending vibration to the amide I mode.

For proteins the amount of the shift is dependent on the type of secondary structure. Often, a shift of 15 cm^{-1} is observed for the weak high-frequency component of β-sheets and of turns.

Bands assigned to disordered structures are shifted by 10 cm^{-1} whereas for all other bands the shift is only a few wavenumbers.

Several factors may contribute to this phenomenon:
(i) The N—H contribution to the amide I mode may differ for the various secondary structures, since the composition of the amide I mode generally depends on the structure of the polypeptide. The size of the band shift in turn will depend on the extent of the N—H contribution to the amide I mode.
(ii) 1H/2H exchange is often incomplete for proteins and this may hold particularly for those ordered secondary structures that show only a small shift.

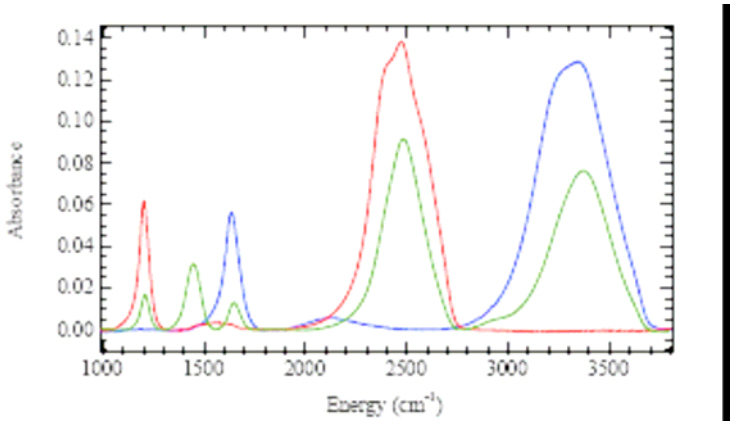

FT-IR spectrum of H_2O (blue), D_2O (red), and 50:50 H_2O:D_2O (green) illustrating the limitations that exist for either solvent since the strong D-O-D, H-O-D, and HO-H bending modes obscures the spectral regions from 1150-1250 cm-1, 1300-1550 cm-1, and 1600-1800 cm-1, respectively.

Time course for hydrogen/deuterium from BPTI,
from 3 minutes to 374 minutes after initiating the exchange.

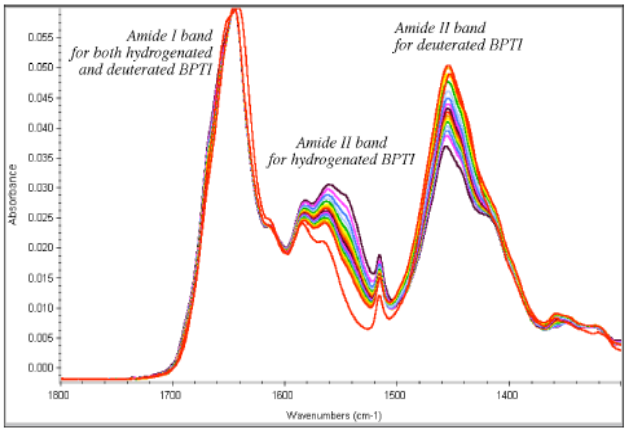

The Amide II band at 1450 cm^{-1} is for deuterated BPTI and is increasing with time. The Amide II band at 1550 cm^{-1} is for hydrogenated BPTI and is decreasing with time. The bottom red spectrum at 1550 cm^{-1} was obtained after complete exchange; the residual absorbency in this region is due to groups on the protein other than the amide group.

The amide I' band of poly-L-lysine in D_2O solution.

Path length, 0.1 mm; concentration, 0.4% by weight. Pure D_2O as reference.

Consecutive spectra displaced by 0.1 scale unit

(upper curve is on scale)

a: random conformation;
b: α-helix;
c: transition between α-helix and antiparallel-chain pleated sheet;
d: antiparallel-chain pleated sheet.

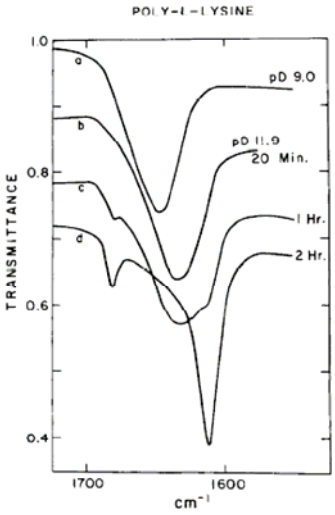

Amide I stretching frequencies

α-helix:	1654 cm^{-1}
β-sheet:	1624, 1631, 1637, 1675
β-turn:	1663, 1670, 1683, 1688, 1694
other:	1645

Protein spectra in ^1H_2O and ^2H_2O in the spectral region between 4000 and 1000 cm^{-1}

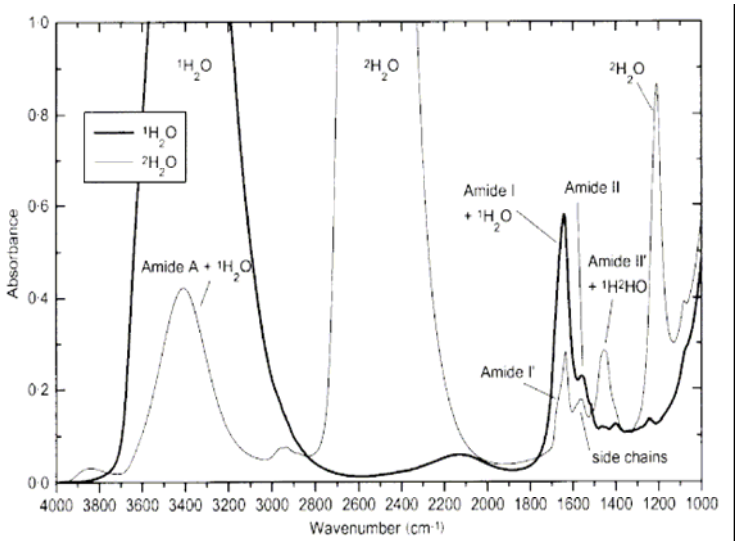

Room temperature IR spectra of the all-β-sheet protein tendamistat in ^1H_2O (bold line) and ^2H_2O (thin line). Sample thickness was approximately 6 and 20 μ for ^1H_2O and ^2H_2O, respectively.

For α-helices there is also evidence for an effect of hydrogen bonding on the vibrational frequency since solvated helices (i.e. helices also forming hydrogen bonds to solvent molecules) absorb approximately 20 cm^{-1} lower than non-solvated helices

The position of the amide I absorbance maximum of different secondary structures correlates with the strength of hydrogen bonding which decreases in the order:
intermolecular extended chains (1610–1628 cm^{-1})
intramolecular antiparallel β-sheets (1630–1640 cm^{-1})
α-helices (1648–1658 cm^{-1})
3_{10}-helices (1660–1666 cm^{-1})
non-hydrogen-bonded amide groups in DMSO (1660–1665 cm^{-1})

For polypeptides there is experimental evidence for an effect of hydrogen bonding on the amide I frequency since the different positions of the main absorption band at 1632 cm^{-1} for poly-L-Ala and at 1624 cm^{-1} for poly-L-Glu were tentatively explained by the stronger hydrogen bonds of the latter.

Determination of global secondary structure- monitoring changes in secondary structure.

Assignment of secondary structure based on position of these bands:

Amide I - C=O stretch (1,630 - 1,660)
Amide II - coupled C-N stretch, N-H bend (1,520 - 1,550)
Amide A - N-H stretch (3,300 H-bonded; 3,400 non-H-bonded)

Amide I stretching frequencies

α-helix: 1654 cm^{-1}
β-sheet: 1624, 1631, 1637, 1675
β-turn: 1663, 1670, 1683, 1688, 1694
other: 1645

The experimental procedure consists of:
- Acquiring the spectrum.
- Fitting the spectrum to the component peaks.
- Determining the area under each peak.
- Calculating the fraction of each secondary structure type.

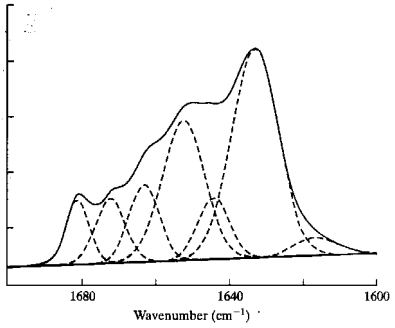

Band fitting

The various secondary-structure components of a protein absorb at different positions in the amide I region of the IR spectrum.

The components largely overlap and a more or less broad and featureless amide I band is observed.

The goal in the curve-fitting approach to secondary-structure analysis is to decompose the amide I band into the various component bands which can then be assigned to the different types of secondary structure.

First the component bands have to be resolved by mathematical procedures of band-narrowing to obtain the band positions, then the amide I band is fitted with bands placed at the positions found and the integrated absorbance of the component bands is calculated. The component bands are assigned.

	Band position in $^1H_2O/cm^{-1}$		Band position in $^2H_2O/cm^{-1}$	
Secondary structure	Average	Extremes	Average	Extremes
α-helix	1654	1648–1657	1652	1642–1660
β-sheet	1633	1623–1641	1630	1615–1638
β-sheet	1684	1674–1695	1679	1672–1694
Turns	1672	1662–1686	1671	1653–1691
Disordered	1654	1642–1657	1645	1639–1654

There are two different approaches to determine the secondary-structure composition of proteins.

The first is based on band narrowing and curve-fitting of the amide I band

The second method uses a calibration set of spectra from proteins with known structure to perform pattern-recognition calculations

Methods of band-narrowing

1.Calculate the second derivative of the spectrum. The linewidth of the second derivative of a band is smaller than that of the original band. Thus, the second derivative can be used to resolve overlapping bands. The minima of the second derivative give the positions of the overlapping components

2. Fourier deconvolution. The line-narrowing principle of Fourier self-deconvolution is the multiplication of the Fourier transform of the original spectrum by a line-shape-dependent function that increases with increasing distance from the centre peak. In the case of deconvoluting Lorentzian lines, an exponential function is used. In this way those regions of the Fourier transform that encode for the fine structure in the original spectrum are weighted more strongly. After back-transformation into a spectrum, components of the spectrum that change strongly with wavenumber (or wavelength or frequency) are amplified: the component bands appear to be 'sharper'.

3. Fine-structure enhancement: a smoothed version of the original spectrum is multiplied with a factor slightly smaller than 1 and subsequently subtracted from the original spectrum, enhancing the fine structure of the spectrum similarly to Fourier self-deconvolution.

Comparison of the band-narrowing techniques second derivative, Fourier self-deconvolution and fine-structure enhancement

(a) IR absorbance spectrum of papain in ^2H_2O recorded at 2 cm^{-1} resolution.
(b) Second derivative of the papain spectrum multiplied by -1. The positive peaks identify the position of several component bands that together constitute the amide I band (1700 to 1610 cm^{-1}). The large peak near 1515 cm^{-1} is the sharp band of the Tyr side-chains.
(c) Fine-structure enhancement (solid line) and Fourier self-deconvolution of the papain spectrum. These two methods give very similar results, the same component bands are identified as with the second derivative.

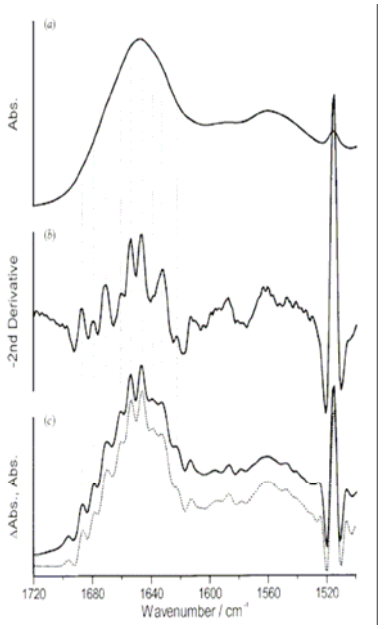

Methods using calibration sets

The second group of methods for secondary-structure analysis, working with factor analysis, partial least squares, or singular value decomposition, avoids some of the problems of the band-fitting approach: the large number of free parameters and the assignment of component bands to specific secondary structures.

A set of proteins with known structure is used as the calibration set which correlates the IR spectra with the secondary structures of the proteins.

The large number of IR spectra of the calibration set of proteins is reduced to a few linearly independent basis spectra. The spectrum of a protein with unknown secondary structure can then be constructed from the basis spectra which reveals the secondary-structure content of that protein.

The calibration set should be diverse and large in order to cover as many different structures as possible. Since there are only a few structures of membrane proteins solved at present, it is difficult to assess the accuracy of the secondary-structure prediction of membrane proteins.

Protein stability

An unfolded protein with a random backbone structure exhibits a broad amide I band centered at approximately 1654 cm^{-1} (in $^{1}H_2O$, room temperature) or 1645 cm^{-1} (in $^{2}H_2O$, room temperature).

The amide I band of an aggregated protein is dominated by a large component at 1620 to 1615 cm^{-1} and a minor component at the high-frequency edge of the amide I region due to the formation of intermolecular β-sheets.

The amide I band of unfolded or aggregated proteins can be distinguished easily from the amide I band of a native protein. Therefore, IR spectroscopy is well suited for protein-stability studies.

Folding and unfolding of proteins can be initiated in various ways: chemically, thermally, and by changing the pressure. Unfortunately, IR spectroscopy of proteins treated with the denaturants urea or guanidinium hydrochloride is hampered by the overlap of their absorption bands with the amide I band of proteins. This overlap can largely be avoided by using [^{13}C]urea.

Temperature-dependent IR absorbance in the amide I region of the small all-β-sheet protein tendamistat.

The midpoint unfolding temperature is 82 ^{0}C.

Experiments are also performed in ^2H_2O solution since the strong band of the ^1H_2O bending vibration is temperature dependent also.

The temperature dependency of the amide I bandwidth, of the wavenumber of maximum absorption, or of the absorbance at appropriate wavenumbers can be used for determination of the transition temperature.

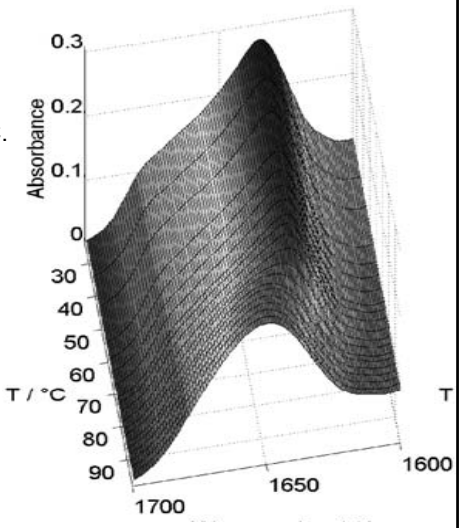

Characteristics of principal infrared absorption bands of the peptide group

Vibration	$\partial\mu/\partial R$	Hydrogen-bonded forms: α Helix Frequency (cm^{-1})	α Helix Dichroism	Hydrogen-bonded forms: β Sheet Frequency (cm^{-1})	β Sheet Dichroism	Non-hydrogen-bonded Frequency (cm^{-1})
N—H stretch	←N—H→ ↔	3,290–3,300	∥	3,280–3,300	⊥	~3,400
Amide I (C═O stretch)	←C═O→ ↔	1,650–1,660	∥	1,630	⊥	1,680–1,700
Amide II	←C—N→ ↗	1,540–1,550	⊥	1,520–1,525	∥	<1,520?

Linear dichroism of the peptide bond. IR spectra of an oriented sample of poly-glutamic acid

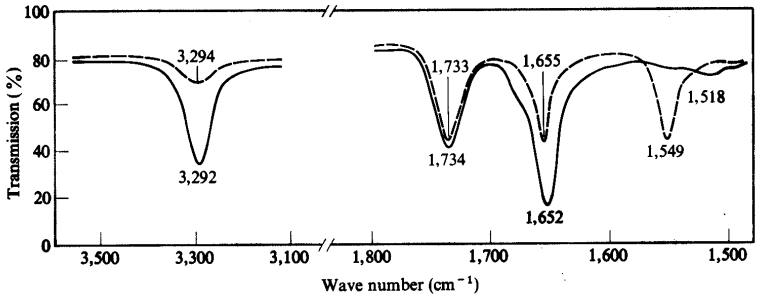

IR radiation polarized parallel (solid line) or perpendicular (dashed line) to the helical axis

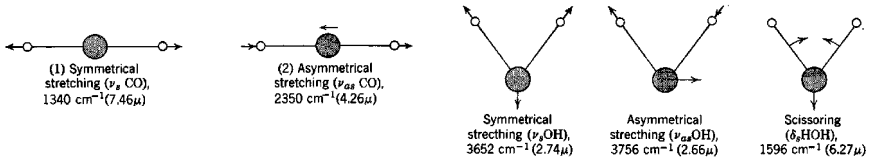

Characteristics of principal infrared absorption bands of the peptide group

		Hydrogen-bonded forms				Non-hydrogen-bonded
		α Helix		β Sheet		
Vibration	$\partial\underset{\sim}{\mu}/\partial R$	Frequency (cm^{-1})	Dichroism	Frequency (cm^{-1})	Dichroism	Frequency (cm^{-1})
N—H stretch	←N—H→ ↔	3,290–3,300	∥	3,280–3,300	⊥	~3,400
Amide I (C═O stretch)	←C═O→ ↔	1,650–1,660	∥	1,630	⊥	1,680–1,700
Amide II	↑ H ←C—N→ ↙ ↓	1,540–1,550	⊥	1,520–1,525	∥	<1,520?

SOURCE: Adapted from J. A. Schellman and C. Schellman, in *The Proteins*, 2d ed., vol. 2, ed. H. Neurath (New York: Academic Press, 1962), p. 1.

The Tyr ring mode near 1517 cm^{-1} is often readily identified in a spectrum because of its small bandwidth. The slight downshift of only a few wavenumbers in ^2H_2O is also characteristic. This mode is an indicator of the protonation state of the Tyr side-chain since the deprotonated form absorbs near 1500 cm^{-1}.

In some cases, the shift of the strong and sharp band of the Tyr aromatic ring-stretching vibration at approximately 1515 cm^{-1} can be analyzed

The Tyr band shifts due to altered hydrogen bonding or changes in π–π interactions and thus indicates alterations of the local environment of the Tyr side-chains.

FTIR has the advantage of resolving the vibrational information originating from the different constituents of the nucleotide into different frequency regions in the FTIR spectrum.

Sugar-phosphate backbone region
Between 1250 cm^{-1} and 1000 cm^{-1}, vibrations along the sugar-phosphate chain give rise to marker bands sensitive to backbone conformation

Sugar region
Between 1000 cm^{-1} and 800 cm^{-1}, changes in the endocyclic torsion angles of the furanose ring give rise to marker bands sensitive to the sugar pucker.

Base-region
Between 1800 cm^{-1} and 1500 cm^{-1} vibrations sensitive to base-pairing and base-stacking interactions appear.

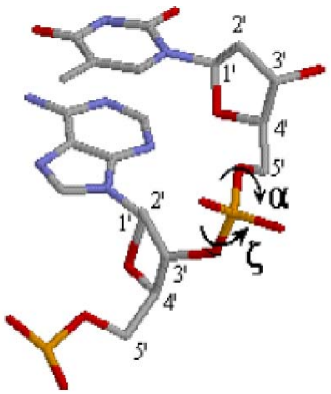

Conformational considerations

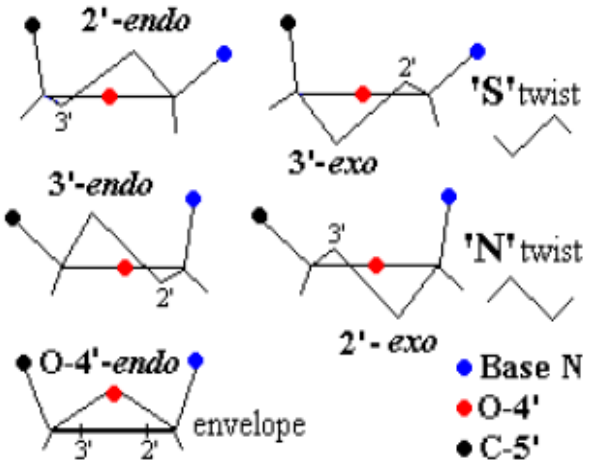

In B-DNA, a strong absorption is seen around 1225 cm^{-1}. This band shifts to 1245-1240 cm^{-1} upon transition into the A-type of conformation.

Absorption bands characteristic of twist type in sugars
N-type (C3'-endo/anti, 870- 862 cm^{-1})
S-type (C2'-endo/anti, 841-834 cm^{-1})

From the relative ratio of the 1740-1600 cm^{-1} and 1600-1550 cm^{-1} multipeak containing bands it can be determined whether the sequences are essentially in a base-paired state.

A single-stranded state would have resulted in approximately similar intensities of the two bands.

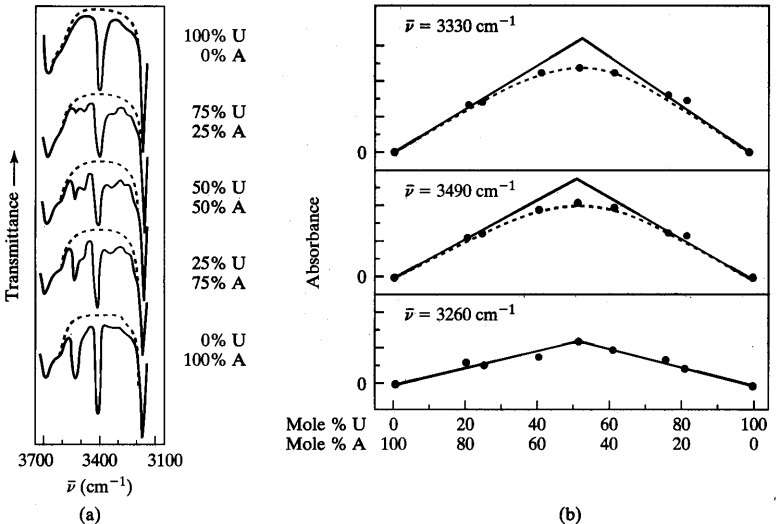

H-bonding in nucleic acids produces bands at 3260, 3330, and 3490 cm^{-1}
9-ethyladenine and 1-cyclohexyluracil were combined at various ratios, and the intensities of these bands were measured.
The maximum in the intensity plot at a stoichiometric levels of the two compounds was consistent with formation of a hydrogen-bonded 1:1 complex.

Tautomerization state of cytosine was first deduced by IR spectroscopy

IR spectrum of cytosine was compared to methylated (and, hence, non-tautomerizing) derivatives having either the keto- or imino forms.

The data clearly demonstrated that cytosine was present in solution in the keto form.

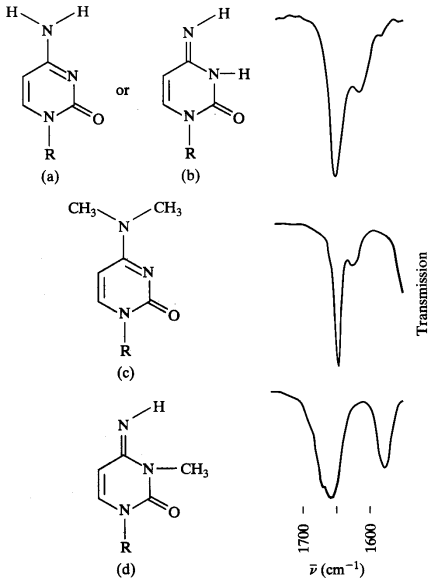

IR Spectroscopy and Nucleic Acids

IR spectroscopy is also useful for nucleic acids.

Each of the four nucleotides has a distinct IR absorption.

IR can be used to monitor double-strand formation.

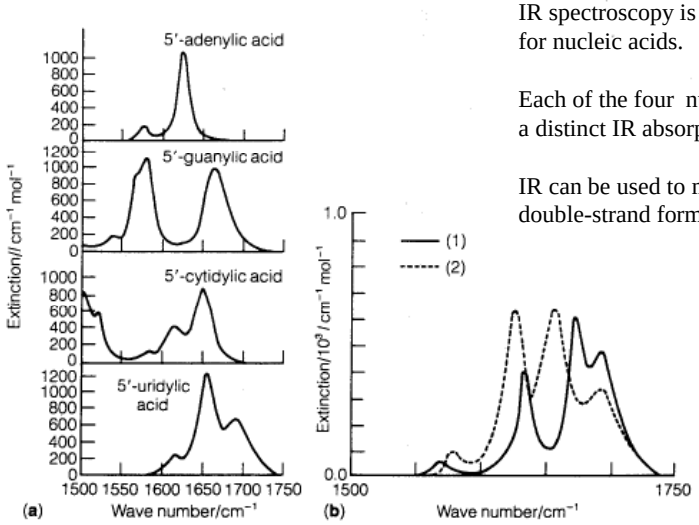

FIGURE 13-9
Infrared spectra of nucleotides and nucleic acids. (a) Spectra in D_2O of four ribonucleotide monophosphates. (b) Spectra in D_2O of poly A and poly U. Curve (1) is for the double-helical poly A · poly U complex. Curve (2) is for the sum of spectra of single-stranded poly A and single-stranded poly U. (From Bloomfield et al., 1974.)

The difference spectra
[(DNA soln + drug)-DNA soln]
DNA band at 968 cm^{-1} as internal reference (due to deoxyribose C–C and C–O stretching vibrations)

no spectral changes (shifting or intensity variations) upon drug–DNA complexation.

guanine at 1710 cm^{-1}
thymine at 1661cm^{-1}
adenine at 1610cm^{-1}
cytosine at 1491 cm^{-1}

The difference spectra showed negative features at 1674 and 1646cm1 due to the loss of intensity of DNA vibrations. This is indicative of a minor, indirect CD-37–DNA interaction via H-bonding.

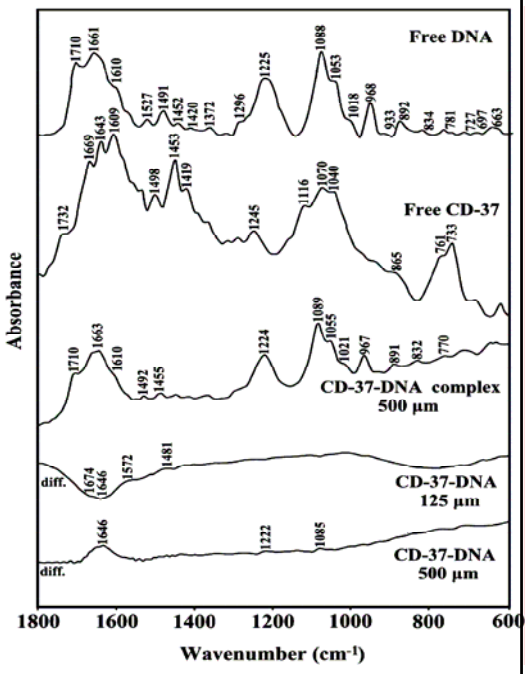

guanine at 1710 cm^{-1}
thymine at 1661cm^{-1}
adenine at 1610cm^{-1}
cytosine at 1491 cm^{-1}

Direct Pt binding to guanine and adenine N7 sites was observed for cisPt–DNA complexes

shifting of the
guanine band
from 1710 to 1706 cm^{-1},
thymine
from 1661 to 1656cm^{-1},
adenine
from 1610 to 1607 cm^{-1}

DNA AND CELL BIOLOGY (2008) 27, 101–107

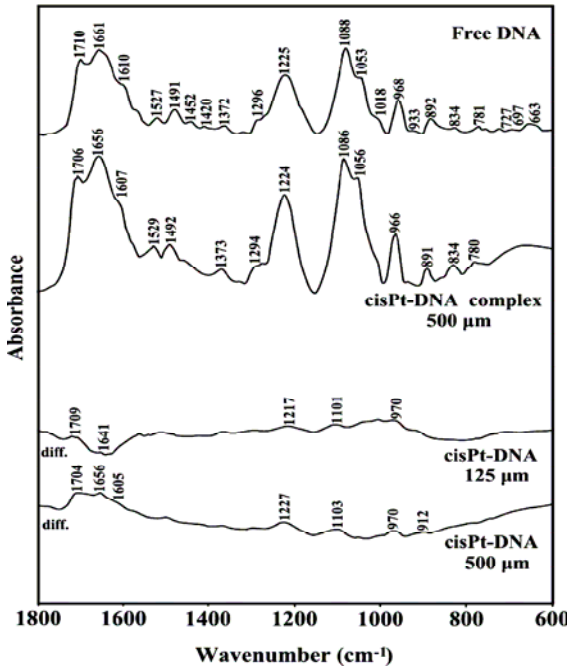

The FTIR employs a Michelson interferometer to simultaneously sample a range of frequencies:

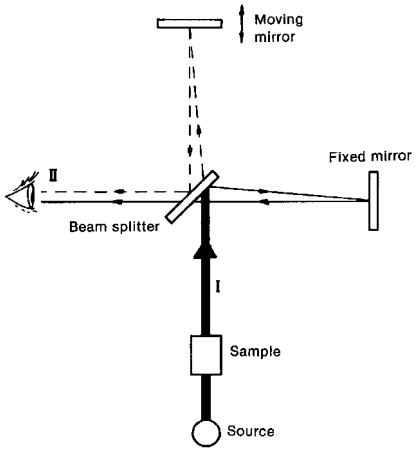

Outputs from fixed and moving mirrors are combined, generating a complex interferogram, as a function of the position of the moving mirror. The nature and extent of interference will depend strongly on frequency and the exact mirror position.
The resulting interferogram is subjected to Fourier analysis, to generate a conventional spectrum – i.e., a plot of intensity versus frequency.

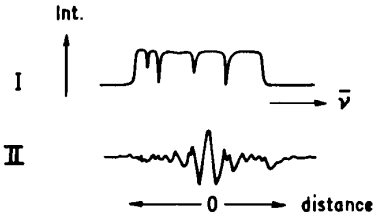

Methods of collecting an infrared spectra interferogram.

The rapidity with which data can be gathered with an FTIR spectrometer, under computer control, permits extensive signal averaging. Since the signal-to-noise ratio increases as the √N,
- It is possible to obtain reliable data on relatively weak signals.
- Accurate solvent subtractions are possible, even in aqueous solution.

Attenuated total reflection (ATR)-FT-IR spectroscopy

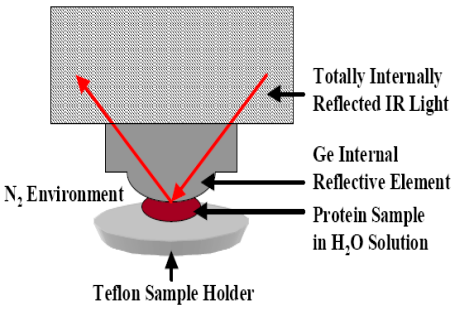

The geometry of the single-pass attenuated total reflection cell is shown. The protein sample is placed in a depression below the Ge crystal.

The index of refraction of Ge and ZnSe crystals are sufficiently high that the infrared light is totally internally reflected.

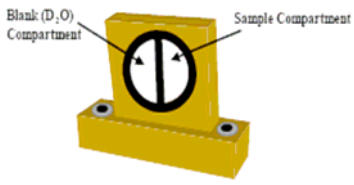

An FT-IR sample cell.
The cell usually used in these experiments consist of two CaF_2 windows and either a 12.5 or 6-micron spacer enclosed with a copper casing.

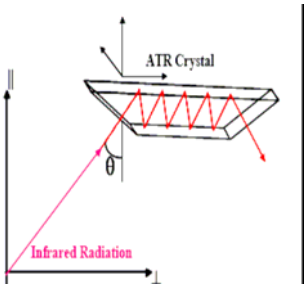

If the angle at which infrared light enters the internal reflective element (also known as an ATR crystal) is greater than the critical angle, then the light will be totally internally reflected. The critical angle is calculated as follows:

$$\theta_{critical} = \sin^{-1}\left(\frac{n_2}{n_1}\right)$$

where n_1 represents the refractive index of the sample and n_2 is the refractive index of the ATR crystal. The refractive index of germanium is 4.0 and the refractive index of a typical protein solution at 1550 cm^{-1} is 1.5, thus the critical angle is 22.0º.

Since the protein is in an N_2 environment, it slowly dehydrates into a concentrated gel state. Rapid scanning can continuously monitor the changes from a fully hydrated state to a concentrated gel state. Concentrating the protein to a gel state yields spectral enhancement such that protein amide bands can be observed simultaneously without performing H_2O subtraction.

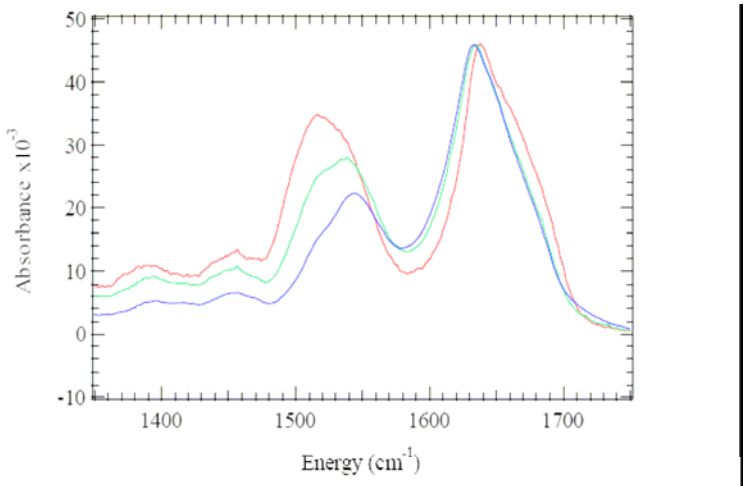

Figure 1.19. Displayed are the spectra of the protein chymotrypsinogen from protein in H_2O solution (blue), to an intermediate state (green), to a gel state (red). These spectra signify the ability to observe any protein denaturation that occurs as a function of gel formation. The amide I position of the hydrated state spectrum is different of that of the intermediate and gel states. Such a significant shift suggests protein denaturation.

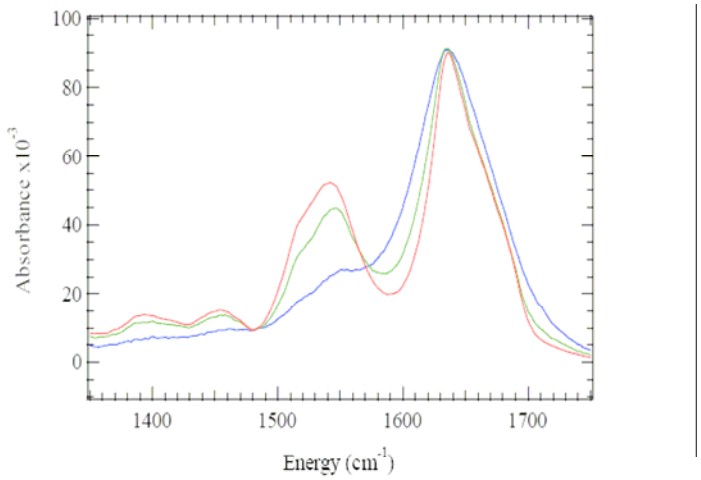

Figure 1.20. Displayed are the spectra of the protein chymotrypsin from protein in H_2O solution (blue), to an intermediate state (green), to a gel state (red). These spectra signify the ability to observe any protein denaturation that occurs as a function of gel formation. The amide I position of gel state spectrum is not different of that of the fully hydrated and intermediate states suggesting that no protein denaturation has occurred.

FTIR Analysis of β-Helical Proteins Biophysical Journal (2000) 78, 994–1000

A 13-residue peptide, KLKLKLELELELG (KLEG), was designed to maximize the opportunity for salt bridges between ionized side chains; this peptide has been demonstrated by electron microscopy to form fibrils. KLEG is thought to form a β-helical structure based on its circular dichroism spectrum

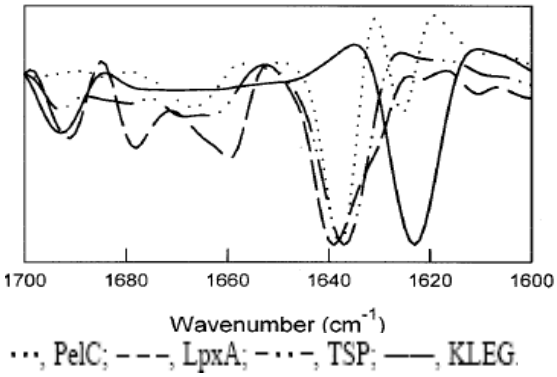

FTIR spectra of the β-proteins and the peptide KLEG.

Second-derivative spectra of the amide I region, showing the major β-structure components in the vicinity of 1638 cm^{-1} for the proteins and 1623 cm^{-1} for KLEG.

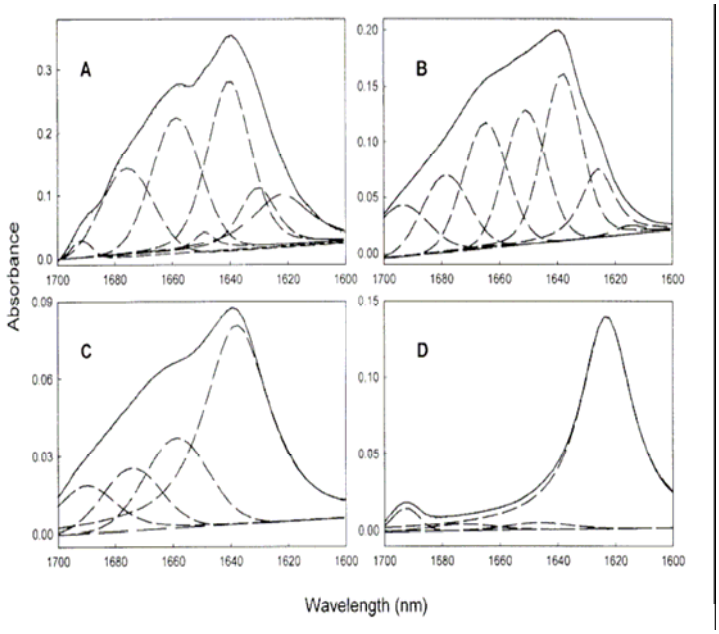

LpxA (*A*), pectate lyase (*B*), P22 tail-spike protein (*C*), and the peptide KLEG (*D*)

TABLE 1 Secondary structure analysis of the amide I peaks in three naturally occurring parallel β-helical proteins, LpxA, pectate lyase C, and P22 tail-spike protein

LpxA		PelC		P22 tail-spike protein		
Peak position	% peak	Peak position	% peak	Peak position	% peak	Protein structure assignment
1692	1	1694	10	1690	11	β or turn
1676	18	1678	13	1674	13	Turn
1659	26	1665	20	1659	20	Loop/turn/bend or α-Helix
1649	2	1651	21			Disordered α-helix
1640	31	1638	26	1638	56	β-Sheet (parallel)
1630	9					β-Sheet
1622	13	1626	10			β-Sheet

The analysis is based on curve-fitting following band deconvolution (see Materials and Methods). The errors are ±1 cm^{-1} for the band positions and ±5% for the peak areas.

TABLE 2 Secondary structural analysis of the amide I peaks for the peptide KLEG

Peak position (cm^{-1})	Percentage peak	Protein structural component
1692	3.8	β or turn
1673	2.5	Turn
1646	2.7	Unknown
1623	91.0	β-Sheet

The errors are ±1 cm^{-1} for the band positions and ±5% for the peak areas.

TABLE 3 Comparison of β-sheet composition (%) from x-ray crystallography and FTIR

	X-ray	1638 cm^{-1}	1624–1630 cm^{-1}	~1692 cm^{-1}
LpxA	27	31	23	1
PelC	29	26	10	10
TSP	37	56	0	11

The three regions of the amide I spectral region in which β-structure is observed are shown. For LpxA and PelC the data suggest that the contributions at frequencies other than 1638 cm^{-1} may be due to the non-β-strand regions of the β-helix. In the case of the tail-spike protein these contributions, especially the turns/loops, are also found at 1638 cm^{-1}.

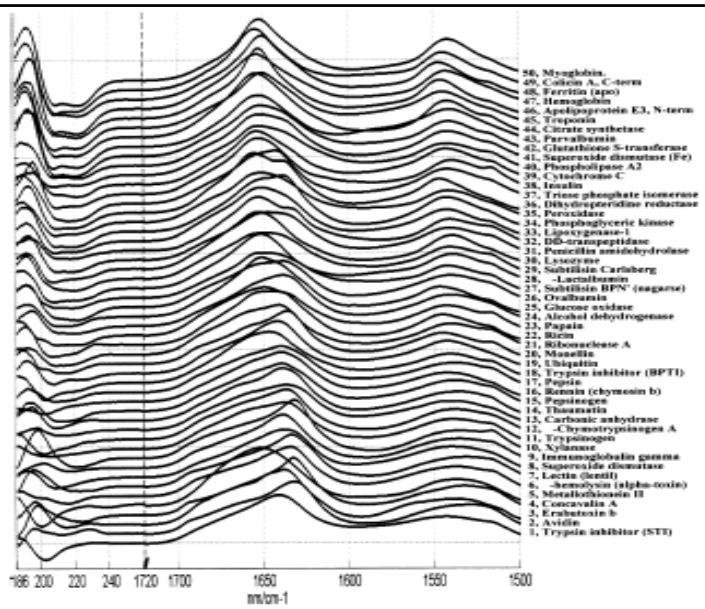

Concatenated CD (186–260 nm) and IR (1720–1500 cm1) spectra of 50 proteins Spectra are been rescaled and offset along the y-axis for a better readability. Proteins are sorted according to their α-helix content.

Raman Spectroscopy

a. An alternative (and complementary) method for studying vibrational transitions.
b. Raman spectroscopy is a light-scattering technique.
c. Raman scattering is inelastic -the scattered radiation has a frequency different from the incident radiation).
d. The phenomenon: a molecule undergoes a vibrational transition coincident with the scattering event. The scattered photon thus emerges with lower (usually) or greater (rarely) energy.

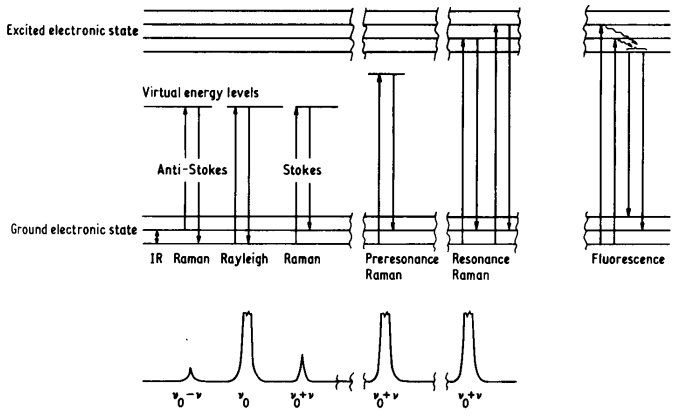

- Raman scattering gives access to vibrations without water peak
- can identify percentages of sugar puckers, glycosidic conformations, ...

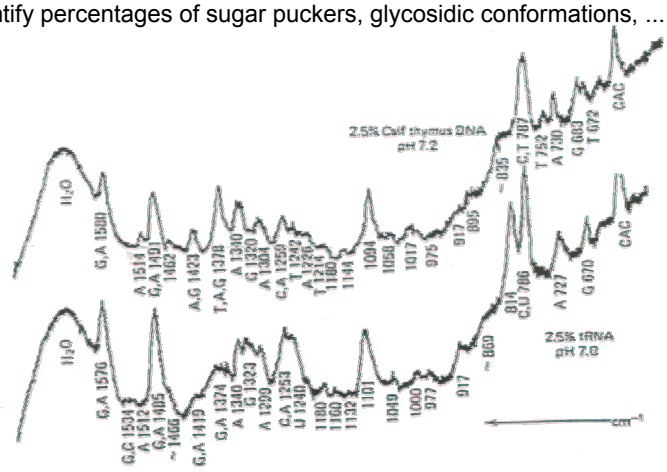

Thus, Raman spectroscopy of dilute aqueous solutions is possible in frequency regions inaccessible to infrared measurements, because the OH-bending vibration which causes intense infrared absorption produces only weak Raman scattering.

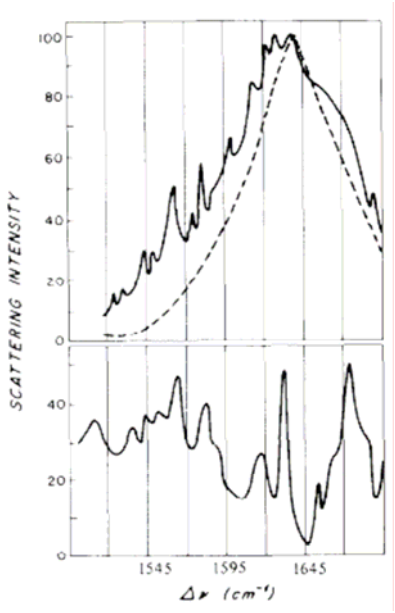

Raman spectrum of water (- - -) and spectrum of an aqueous solution of poly-L-lysine (1 mg/ml) in the antiparallel β-conformation (solid line).

Lower panel: Raman spectrum of a 1 mg/ml solution of β-structured poly-L-lysine. with the water contribution subtracted out.

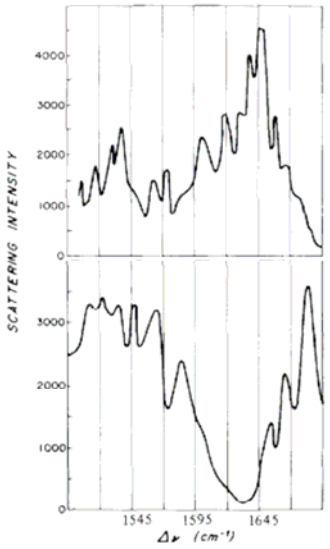

Upper panel: Raman spectrum of α-helical poly-L-lysine.

Lower panel: Spectrum of "unordered" poly-L-lysine.

Raman spectrum of P22 virus at a concentration of 80 μg/mL (sample volume of just 2 μL) Incident wavelength: 514.5 nm

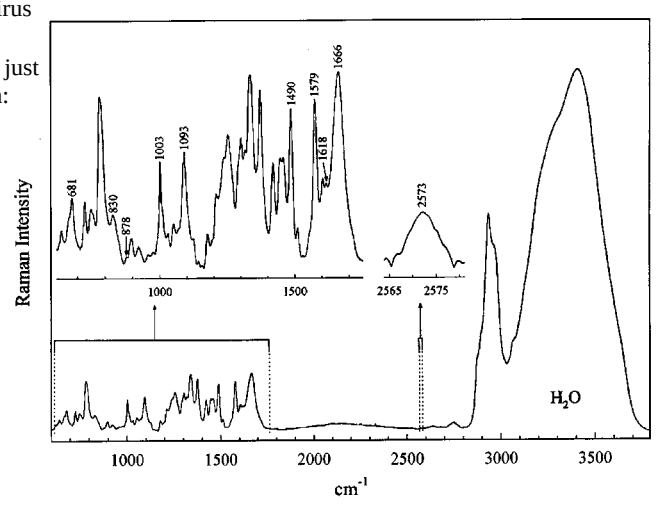

Broad water peak at 3000-3700 cm^{-1}.

peak at 2950 includes the aliphatic C-H transitions of the protein and DNA.

The peak at 2573 is the -SH group of the Cys-405 of the capsid protein.

Raman spectroscopy requires more complex instrumentation, data acquisition times are generally longer, and the signal-to-noise is generally inferior to FTIR methods.

Predicted position of Raman lines:

$$\lambda(\text{cm}) = \frac{1}{\frac{1}{\lambda_o(\text{cm})} - \nu'(\text{cm}^{-1})}$$ where λ_o is the wavelength (in cm) of incident light,

and ν' is the frequency of the vibrational transition in wavenumbers

With an incident wavelength of 514 nm, where would the water stretching band at 3500 cm^{-1} appear?

$$\lambda = \frac{1}{\frac{1}{5.14\times10^{-5}} - 3500} = 6.27\times10^{-5}\ \text{cm} = 627\ \text{nm}$$

	DNA sequence	%G + C	X-ray structure	NMR structure
CAT	[C-A-T-A-T-G-C-A-T-A-T-G]$_2$	33		
22	[C-A-T-**G-G-C-C**-A-T-G]$_2$	60	*B*-form[16]	*B*-form[17]
33	[C-A-T-**G-G-G-C-C-C**-A-T-G]$_2$	67	*A*/*B*-form[18]	*B*-form[20]
44:1	[C-A-T-**G-G-G-G-C-C-C-C**-A-T-G]$_2$	71		
44:2	[A-**G-G-G-G-C-C-C-C**-T]$_2$	80	*A*-form[21]	
44:3	[T-**G-G-G-G-C-C-C-C**-A]$_2$	80		

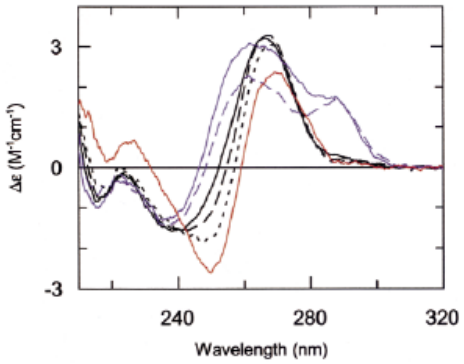

Figure 1. CD spectra of CAT (—, red), 22 (------), 33 (– – –), 44:1 (—), 44:2 (—, blue), and 44:3 (– – –, blue). Recorded at 4 °C in buffer containing 0.1 M NaCl.